



A bifunctional electrochemical aptasensor based on AuNPs-coated ERGO nanosheets for sensitive detection of adenosine and thrombin

Hongmei Yang^{1,2} · Peiyu Hu^{1,2} · Jing Tang¹ · Ying Cheng¹ · Fang Wang^{1,2} · Zilin Chen^{1,2}

Received: 24 August 2020 / Revised: 4 November 2020 / Accepted: 7 February 2021 / Published online: 20 February 2021
© The Author(s), under exclusive licence to Springer-Verlag GmbH, DE part of Springer Nature 2021

Abstract

A simple and sensitive bifunctional electrochemical aptasensor for detection of adenosine and thrombin has been developed using gold nanoparticles–electrochemically reduced graphene oxide (AuNPs-ERGO) composite film-modified electrode. Firstly, the reduced graphene oxide film and AuNPs were sequentially immobilized on glassy carbon electrode (GCE) surface. Secondly, thrombin aptamer was immobilized on the modified electrode. Finally, adenosine aptamer was hybridized with it to serve as a recognition element and methylene blue (MB) as electrochemical signal indicator. In the presence of adenosine or thrombin, the sensor recognized it and a conformational change was induced in aptamer, resulting in decrease of the peak current of MB. The linear relation between concentration of adenosine or thrombin and peak current of MB allowed quantification of them. Thanks to the special electronic characteristic of AuNPs-ERGO composite film, sensitivity of sensor was greatly improved. Under optimal conditions, the proposed aptasensor presented an excellent performance in a linear range of 25 nM to 750 nM for adenosine and 0.5 nM to 10 nM for thrombin. Detection limits were estimated to be 8.3 nM for adenosine and 0.17 nM for thrombin, respectively. Moreover, dual-analyte detection of adenosine and thrombin was achieved without potentially increasing the complexity and cost of the assay.

Keywords Aptasensor · Gold nanoparticles · Electrochemical-reduced graphene oxide · Adenosine · Thrombin

Introduction

Quantitative detection of small molecules and proteins have attracted great attention in biomedical fields, including disease diagnosis and clinical medicine. Adenosine, as an endogenous nucleoside modulator, is one of the most important small molecules. It takes part in regulating smooth muscle contraction, blood flow, neurotransmission, renal hemodynamics, and release of renin [1]. Thrombin is the last protease in the

coagulation cascade, which acts to cleave soluble fibrinogen to insoluble fibrin, forming the fibrin gel either of a physiologic plug or a pathologic thrombus [2]. As a hormone, thrombin can also regulate platelet aggregation, endothelial cell activation, and other crucial responses in vascular biology [3]. So it plays significant roles in various pathological and physiological processes, such as angiogenesis, tumor growth hemostasis, blood coagulation cascade, and arterial thrombosis [4]. Thus, the detection of adenosine and thrombin is of great value in clinical research and disease diagnosis.

In recent years, several methods have been developed to detect adenosine or thrombin, including photo-induced enhanced Raman spectroscopy, high-performance liquid chromatography, fluorescence, aptamer-based optical sensing, affinity chromatography, mass spectrometry, enzymatic assays, and electrochemical biosensor [5–8]. Electrochemical biosensors have been well developed due to the advantages of low cost, easy operation, good portability, excellent flexibility, and high sensitivity. Generally, there are two main approaches to increase the sensitivity of electrochemical biosensors in the detection of small molecules and proteins. One is to improve electronic characteristics of electrode, such as enhancing

Hongmei Yang and Peiyu Hu contributed equally to this work.

✉ Fang Wang
fwang@whu.edu.cn

✉ Zilin Chen
chenzl@whu.edu.cn

¹ Key Laboratory of Combinatorial Biosynthesis and Drug Discovery, Ministry of Education, Hubei Province Engineering and Technology Research Center for Fluorinated Pharmaceuticals, Wuhan University School of Pharmaceutical Sciences, Wuhan 430071, China

² State Key Laboratory of Transducer Technology, Chinese Academy of Sciences, Beijing 100080, China

electron transfer rate and increasing electrode effective surface area [9]. Chemical materials, such as high polymers, carbon nanotubes, and nanoparticles, are often used to modify electrode surface in electronic characteristic improvement. Graphene, a two-dimensional new carbon material, has drawn great attention because of its excellent electron mobility, high surface-to-volume ratio, and remarkable chemical stability. A major drawback of graphene is natural hydrophobicity, leading to its poor solubility in polar solvents. In order to conquer this challenge, graphene can be oxidized to be graphene oxide (GO) before further use. However, the oxidation process introduces sp^3 hybridized carbon into GO structure, which tends to decrease the electrical conductivity due to disruption of sp^2 network [10, 11]. Then, GO can be chemically or electrochemically reduced to be reduced graphene oxide for the purpose of electrical conductivity improvement. Compared with chemically reduced graphene oxide (RGO), electrochemically reduced graphene oxide (ERGO) is convenient, eco-friendly, and more efficient for electron transfer, which is favorable for application in biosensor [12]. In addition, a lot of researches have shown that using various metal nanoparticles as coat on graphene can further improve the electronic characteristic of sensor [13–15]. Among numerous metal nanoparticles, gold nanoparticles (AuNPs) have been widely applied to biosensors because of their unique electronic properties and excellent biocompatibility. They can provide a suitable microenvironment for biomolecules immobilization and facilitate electron transfer between molecules and electrode [16, 17]. So, AuNPs-coated ERGO nanosheets might be a good choice for electrode modification. It can not only enhance the electrical conductivity but also improve the biocompatibility and holds great promise in construction of biosensor.

The other factor in sensitivity enhancement of sensor is selection of target recognition element. It is necessary to choose molecules with high selectivity and excellent biocompatibility. Presently, aptamers are popular in biosensor fabrication as recognition elements [18–21]. They are short nucleic acid oligomers selected from random nucleic acid libraries via an in vitro evolution process termed systematic evolution of ligands by exponential enrichment (SELEX) [22–24]. Aptamers have been considered as “chemical antibodies” due to their capability of target recognition with high affinity and specificity toward a wide range of molecules, including proteins, metal ions, and other organic or inorganic molecules [25, 26]. Moreover, aptamers possess a series of advantages over antibodies, such as simple synthesis, easy modification, excellent stability, and low immunogenicity [27, 28]. Based on these characteristics, we developed a simple and sensitive bifunctional electrochemical aptasensor for the determination of adenosine and thrombin.

The proposed method herein was based on gold nanoparticles–electrochemically reduced graphene oxide (AuNPs-ERGO) composite film modified electrode. GO was

firstly immobilized onto GCE and then electrochemically reduced. After that, AuNPs were electrodeposited on ERGO film at electrode surface, which could not only further enhance the electron transfer rate but also facilitate grafting aptamers, and thus increasing detection sensitivity. Furthermore, two complementary aptamers were ingeniously designed to achieve dual-analyte detection and also to improve the selectivity of sensor. Owing to this strategy, adenosine and thrombin could be specifically detected with a low detection limit.

Experimental

Reagents and apparatus

Adenosine, guanosine, uridine, methylene blue (MB), and 1-hexanethiol (MCH) were all supplied by Aladdin Reagent Co. Ltd. (Shanghai, China). Thrombin, bovine plasma albumin (BSA), and lysozyme were ordered from Sigma-Aldrich (Shanghai, China). Graphite powder was purchased from Alfa Aesar Chemical Co. Ltd. (Shanghai, China). Chloroauric acid ($\text{HAuCl}_4 \cdot 4\text{H}_2\text{O}$) was obtained from Sinopharm Chemical Reagent Co. Ltd. (Shanghai, China). Potassium sulfate (K_2SO_4), phosphorus pentoxide (P_2O_5), potassium permanganate (KMnO_4), and polyvinylpyrrolidone (PVP) were all ordered from Macklin Biochemical Co. Ltd. (Shanghai, China). All reagents were used as received in analytical grade. All samples were prepared with 10 mM Tris-HCl (pH 7.4) buffer and stored at 4 °C before use. Deionized water was purified by a Milli-Q water purification system (MA, USA). The deionized water and buffer used were filtered through a 0.22- μm membrane.

All oligonucleotides were synthesized by TaKara Biomedical Technology Co. Ltd. (Beijing, China). The sequences of two oligomers are given as follows:

Thrombin aptamer (noted as TBA): 5'-SH-(CH_2)₆-AGT CCG TGG TAG GGC AGG **TTG GAC CTT CC**-3'

Adenosine aptamer (noted as ABA): 5'-ACC TGG GGG AGT ATT GCG GAG **GAA GGT CCA AC**-3'

In these aptamers, the complementary parts are in bold and the recognition parts are in italic.

All electrochemical experiments were carried out on CHI 750D electrochemical workstation (Shanghai CH Instruments Co, China) in a conventional three-electrode system. A bare GCE or modified GCE was used as working electrode. A saturated calomel electrode (SCE) and a platinum wire were used as the reference electrode and auxiliary electrode, respectively. The surface morphology and structure of composite film (AuNPs-ERGO) and ERGO nanosheets at modified electrodes were observed by scanning electron microscopy

(SEM), and was performed with a Hitachi X-650 microscopy (Japan).

Synthesis of GO and RGO

GO was synthesized by a modified Hummers method [29]. Graphite powder (1.50 g, 325 mesh) was added into a mixture containing K_2SO_4 (1.25 g), P_2O_5 (1.25 g), and concentrated H_2SO_4 (6.0 mL) at 80 °C for 4.5 h, and then the mixture was cooled to room temperature, diluted with 0.25 L of water, and stood overnight. After the mixture was filtered and washed with water using a 0.22- μ m nylon millipore filter. The product was air-dried overnight, and it was added to cold (0 °C) concentrated H_2SO_4 (60.0 mL), and then $KMnO_4$ (7.5 g) was added dropwise with temperature controlled below 20 °C. The mixture was stirred at 35 °C for 2 h. One hundred and twenty-five milliliters of deionized water were added to prevent temperature from exceeding 50 °C for further reaction for 2 h. Following this, 350 mL of deionized water and 10 mL of 30% H_2O_2 were added into the mixture, producing a brilliant yellow color along with bubbling. Then, filtration and washing were sequentially carried out by 500 mL of HCl (1:100) and 500 mL of deionized water. The obtained product was dried at 50 °C overnight, and exfoliation was achieved by sonicating a 1 mg/mL dispersion for 30 min.

RGO was prepared according to literature with minor modification [30]. In brief, the prepared GO dispersion was diluted to a 0.5-mg/mL aqueous suspension and sonicated for 30 min. Then, GO suspension and 4 mg/mL polyvinylpyrrolidone (PVP) aqueous solution were mixed to 10 mL at a ratio of 1:1 (v/v) and stirred at 50 °C for 12 h. When it was cooled to room temperature, 3.5 μ L of hydrazine solution and 40 μ L of ammonia water were added into above solution with stirring for a few minutes. The mixture was then transferred to an oil bath and heated to 95 °C for 1 h. Finally, a black dispersion was obtained and it was washed and purified by centrifugation, then the precipitate was redispersed in water to form a 1 mg/mL dispersion for further use.

Fabrication of electrochemical aptasensor

Before modification, GCE (3 mm of diameter) was sequentially polished to mirror-like surface with 1.0-, 0.3-, and 0.05- μ m alumina slurries on different roughness cloths and then sonicated in ethanol and deionized water, separately. After being blow-dried with nitrogen, 5 μ L of GO dispersion (1 mg/mL) was dropped onto the GCE surface, and dried at room temperature for 5 h. A graphene oxide-modified electrode (GO/GCE) was obtained. Next, the modified electrode was immersed into 5 mL of 0.1 M phosphate buffer solution (pH 4.6, 10 mM Na_2HPO_4 - NaH_2PO_4 containing 0.1 M NaCl), and nitrogen was introduced to remove dissolved oxygen in buffer for 15 min. Then, electrochemical reduction

was performed by cyclic voltammetry (CV) in the potential range from 0.0 to -1.2 V at a scan rate of 50 mV/s with nitrogen protection [31]. The electrode was rinsed with deionized water and dried under nitrogen stream. Upon electrochemical reduction, a grayish dark film was visible on GCE surface and electrochemically reduced graphene oxide nanosheets-modified electrode (ERGO/GCE) was obtained.

Following this process, ERGO/GCE was immersed in 10 mM $H AuCl_4$ solution and AuNPs were electrochemically deposited on the ERGO/GCE surface using amperometry technique at a potential of -0.2 V. The modified electrode was designated as AuNPs-ERGO/GCE. Then, 5 μ L of 8.6 μ M TBA was dropped onto the electrode surface and kept at 4 °C for 16 h. After that, the electrode was treated with 1 mM MCH for 1 h to eliminate nonspecific binding on electrode surface. The hybridization reactions were carried out by casting 5 μ L of 7.8 μ M ABA onto the electrode surface, followed by incubation for 1.5 h. After rinsed with washing buffer and dried using a mild nitrogen stream, the aptasensor was obtained.

Determination of adenosine and thrombin

Fabricated aptasensor was firstly soaked in 4 mL of 20 μ M MB solution for 10 min under gently stirring. Then, MB modified electrode was incubated in different concentrations of thrombin or adenosine for 1 h. Followed by thoroughly washing, the electrochemical response of aptasensor was recorded by differential pulse voltammetry (DPV) from 0.0 to -0.6 V and tris hydroxymethyl aminomethane hydrochloride (Tris-HCl) buffer (10 mM, pH 7.4) was used as supporting electrolyte. It should be noted that the supporting electrolyte was deoxygenated with nitrogen bubbling for at least 10 min prior to electrochemical measurements. Electrochemical impedance spectroscopy (EIS) experiments were performed in 0.1 M KCl aqueous solution with 5 mM $[Fe(CN)_6]^{3-/4-}$.

Results and discussion

Principle of aptasensor

An aptasensor was designed for adenosine and thrombin detection. Its signal output comes from target induced structure-switching of aptamer and signal amplification from AuNPs-coated ERGO nanosheets platform. Principle of this aptasensor was then described in details. Thrombin aptamer (TBA) and adenosine aptamer (ABA) are employed as recognition probes. TBA with a thiolated modification is composed of a sequence complementary to ABA (bold) and a thrombin aptamer sequence (italic). ABA also contains a sequence complementary to TBA (bold) and a sequence responsible for adenosine recognition (italic). As illustrated in Fig. 1, ERGO

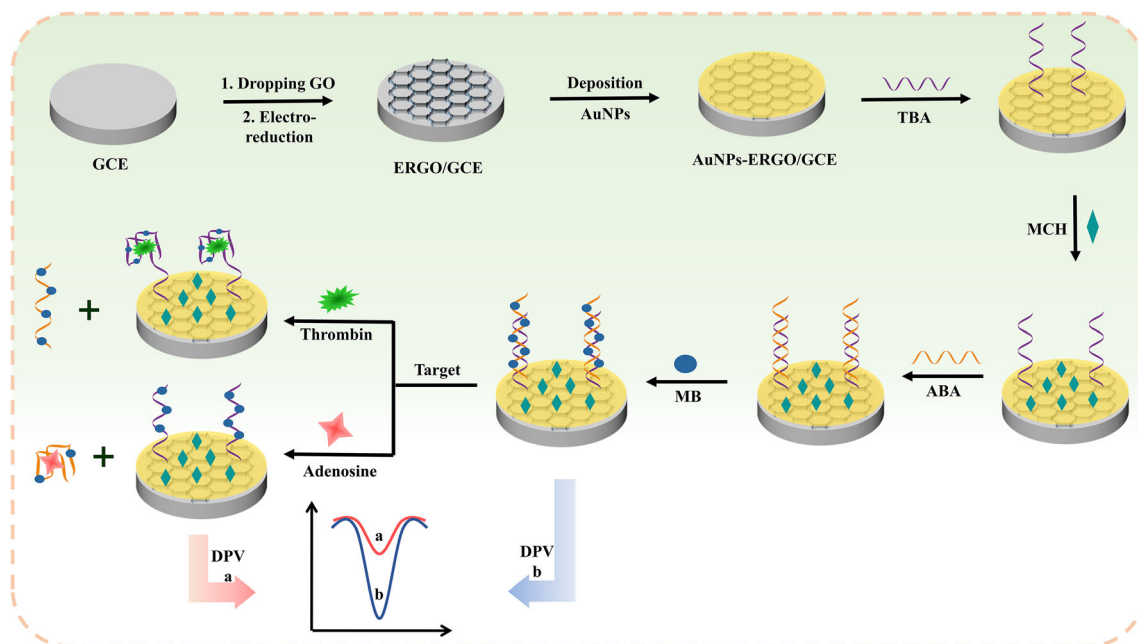


Fig. 1 Schematic illustration of the stepwise fabrication of aptasensor and target detection

nanosheets are firstly coated on GCE and then electrochemically reduced, which can not only accelerate the surface electron transfer rate but also provide a large surface area for AuNPs deposition. Then, AuNPs are electrodeposited on ERGO/GCE for immobilization of TBA by Au-S bond and further enhancement of aptasensor conductivity. Following immobilization of TBA on AuNPs-ERGO/GCE, ABA is added to form double-strand DNA (dsDNA) with TBA by hybridization. MB as a signal indicator is incubated with them and can abundantly adsorb on recognition probes via specific interaction with guanine base in DNA. The more amount of MB, the larger current response. Therefore, the current response will reach a maximum when there is a saturation of combination between MB and aptamers (curve b). In the presence of target (adenosine or thrombin), recognition probe will have a conformational alteration to form G-quadruplex, resulting in MB releases from the modified electrode and then the current response decreases (curve a). The higher target concentration, the lower signal value. Thus, signal response is linearly related to the concentration of target and this aptasensor is allowed to detect adenosine and thrombin.

Characterization of modified electrode

The effects of GO, RGO, and ERGO on improving electrode conductivity were evaluated by cyclic voltammetry (CV). Furthermore, AuNPs were also electrodeposited onto the modified electrodes in order to test the performance of integrated sensing platform. Cyclic voltammograms of $[\text{Fe}(\text{CN})_6]^{3-/4-}$ at these electrodes are depicted in Fig. 2, a couple of well-defined redox peaks for bare GCE can be

observed in curve b. Apparently, curve a shows that AuNPs-ERGO film modified electrode could decrease the peak current of $[\text{Fe}(\text{CN})_6]^{3-/4-}$. Due to disruption of sp^2 network, a large amount of oxygen-containing functional groups in GO would decrease the electron transfer rate between GCE and $[\text{Fe}(\text{CN})_6]^{3-/4-}$, even though AuNPs possess excellent conductivity [11, 17]. When AuNPs-RGO (curve c) or AuNPs-ERGO (curve d) composite film was modified on GCE, the peak currents were obviously enhanced, and currents at AuNPs-ERGO/GCE are larger than that at AuNPs-RGO/GCE. This may be attributed to the fact that ERGO film is more uniform and completely reduced than that dropping-formed RGO film.

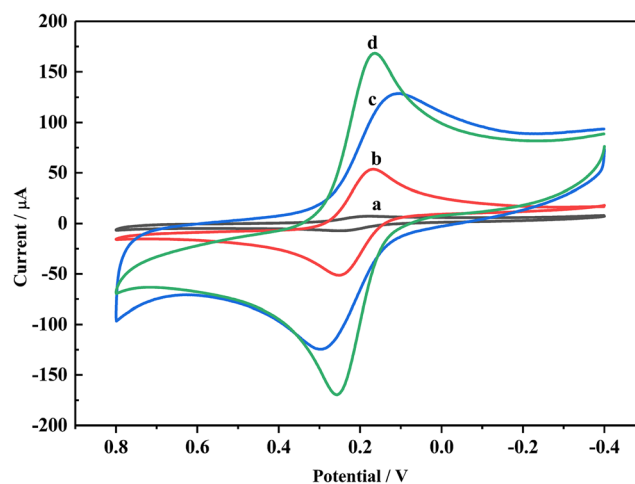
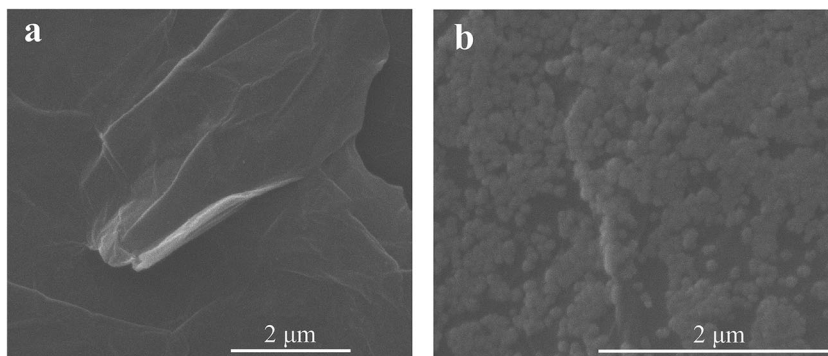


Fig. 2 Cyclic voltammograms of **a** AuNPs-GO/GCE, **b** bare GCE, **c** AuNPs-RGO/GCE, **d** AuNPs-ERGO/GCE in 0.1 M KCl solution with 5 mM $[\text{Fe}(\text{CN})_6]^{3-/4-}$

Fig. 3 SEM images of **a** ERGO/GCE and **b** AuNPs-ERGO/GCE



Scanning electron microscopy (SEM) was used to characterize the morphologies of modified films at GCE surface. The SEM images of ERGO nanosheets and AuNPs-ERGO composite film modified electrodes are shown in Fig. 3. The surface of ERGO modified GCE exhibits rippled and crumpled sheets-like waves (Fig. 3a), indicating that ERGO nanosheets can increase the surface area of electrode. After AuNPs were electrodeposited onto the modified electrode to form AuNPs-ERGO composite film (Fig. 3b), a golden yellow film on the electrode surface could be observed by naked eye. The AuNPs layer looks dense and disperses homogeneously on the surface of ERGO, which can further increase the surface area of electrode. These SEM images revealed a successful modification of AuNPs-ERGO/GCE.

Electrochemical impedance spectroscopy (EIS) is an effective tool to reflect the surface properties of modified electrode. In order to further investigate the electronic properties of AuNPs-ERGO film at electrode surface, Nyquist plots were recorded at different modified electrodes by EIS in 0.1 M KCl aqueous solution containing

5 mM $[\text{Fe}(\text{CN})_6]^{3-/4-}$. The data are shown in Fig. 4a. Generally, Nyquist plot comprises a semicircular part at high-frequency region and a straight linear part at low-frequency region. High-frequency region is controlled by electrode reaction kinetics (charge transfer process), and low-frequency region is controlled by diffusion of reactants or products in the electrode reaction. The electron transfer resistance (R_{et}) can be estimated from the semi-circle diameter of Nyquist plot [32]. Apparently, it can be found that the impedance responses of $[\text{Fe}(\text{CN})_6]^{3-/4-}$ at different modified electrodes show different characteristics. A small semicircle at high frequency can be observed at bare GCE (curve ii). The diameter of semicircle is larger than that at bare GCE after GO film was modified on the surface of bare GCE (curve i), indicating great increase of the R_{et} values of GO/GCE due to poor conductivity of GO. On the contrary, bare gold electrode could distinctly enhance the electron transfer rate because of its excellent electrical characteristics. So, its Nyquist plot exhibits a complex line with a small semicircle at high

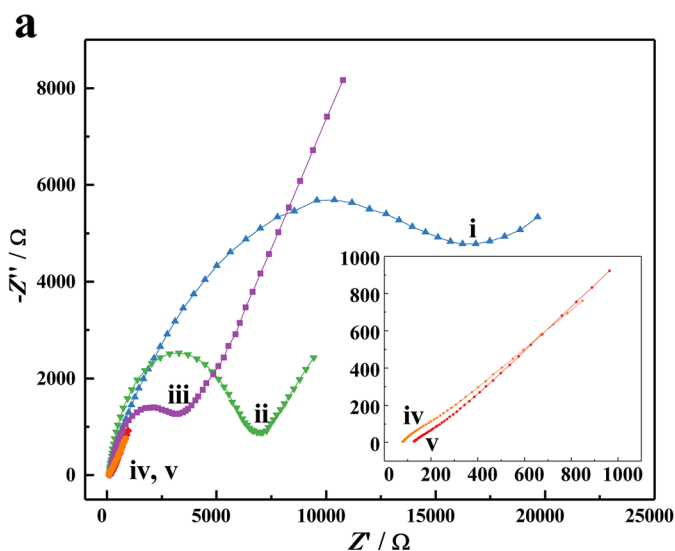
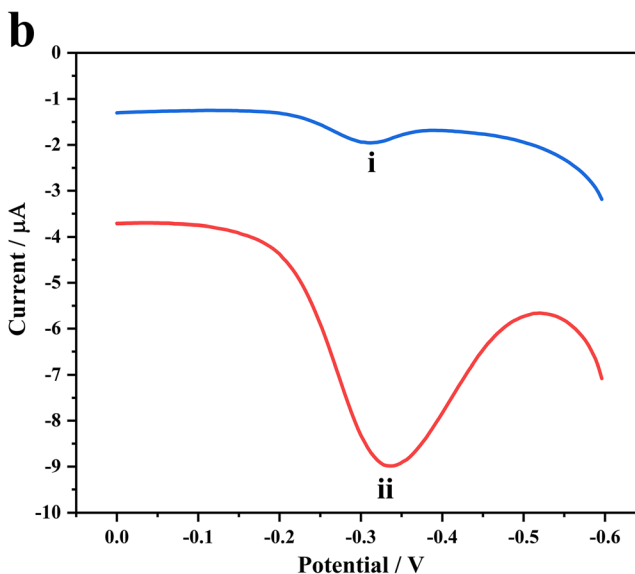


Fig. 4 a Nyquist diagram for the EIS measurements of (i) GO/GCE, (ii) bare GCE, (iii) bare gold electrode, (iv) ERGO/GCE, (v) AuNPs-ERGO/GCE in the presence of 5 mM $[\text{Fe}(\text{CN})_6]^{3-/4-}$. **b** Differential pulse



voltammograms of 20 μM MB at (i) TBA/AuNPs/GCE and (ii) TBA/AuNPs-ERGO/GCE in 10 mM Tris-HCl (pH 7.4)

frequency and almost a straight line at low frequency (curve iii). As we expected, a complex nonlinear line appears almost without semicircle at ERGO/GCE (curve iv), showing that the R_{ct} value decreased significantly. When AuNPs were further deposited on the surface, only an almost straight line can be observed (curve v). Change of R_{ct} value of different electrodes further confirmed successful modification of ERGO and AuNPs, and quite fast electron transfer between AuNPs-ERGO composite film and GCE.

Differential pulse voltammetry (DPV) was applied to measure MB signal at AuNPs/GCE and AuNPs-ERGO/GCE after the electrodes were incubated with TBA. The results are shown in Fig. 4b. Reduction peak current of MB is directly related to amount of TBA on electrode surface. The peak current of MB at TBA/AuNPs-ERGO/GCE (curve ii) is much larger than that at TBA/AuNPs/GCE (curve i), demonstrating that more TBA have been assembled on the surface of AuNPs-ERGO/GCE. Meanwhile, it was confirmed that GO was successfully reduced to ERGO on electrode and ERGO could improve the effective surface area and conductivity of electrode.

Optimization of ERGO and AuNPs film

Experimental parameters involved in preparation of ERGO and AuNPs film were optimized by DPV. Thick of ERGO nanosheets on electrode is a key factor for signal enhancement. It is mainly depended on the number of voltammetric cycles for ERGO preparation. The DPV peak current increased with voltammetric cycles ranging from 5 to 10, and then the current decreased when further increasing cycles. The maximum peak current appeared at 10 cycles. This may be caused by the increase of ERGO thickness that

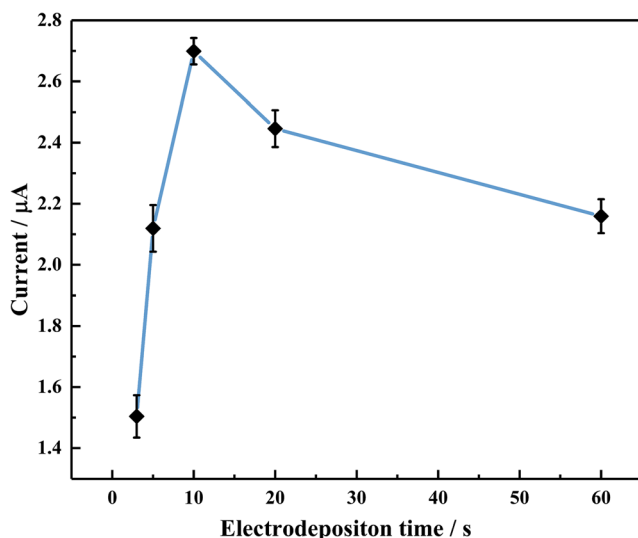


Fig. 5 Optimization of electrodeposition time for AuNPs

Table 1 Performance comparison of different analytical methods for the detection of adenosine or thrombin

Method	Linear range of A (nM)	LOD of A (nM)	Calibration equation	Linear range of T (nM)	LOD of T (nM)	Calibration equation	Refs.
FL	500–7000	103.4	$Y = 360.6 + 29X$	50–900	8.4	$Y = 183.3 + 0.32X$	[6]
FL	0–12.5	0.39	$Y = 0.02226 + 0.0146X$	2–25	2.2	$Y = 0.0110 + 0.0765X$	[35]
FL	1.0×10^3 – 1.2×10^5	2.0×10^2	$Y = 14.6 + 1769.7 \times 10^4 X$	–	–	–	[36]
FL	1.0×10^3 – 1.0×10^5	4.2×10^2	–	–	–	–	[37]
SERS	5–500	5	–	–	–	–	[38]
SERS	2–250	2	–	–	–	–	[39]
EC	–	–	–	100–1000	98	$Y = 4.648 + 0.656X$	[40]
FL	–	–	–	2.0×10^{-5} – 5.0×10^4	12	–	[41]
FL	–	–	–	10–2000	8.1	–	[42]
LC-MS/MS	–	–	–	0.5–50	0.3	$Y = 1.497 \times 10^{-2} X - 5.880 \times 10^{-3}$	[43]
EC	25–750	8.3	$Y = 2.411 - 0.001X$	0.5–10	0.17	$Y = 2.303 - 0.104X$	This work

FL, fluorescence; SERS, surface-enhanced Raman spectroscopy; EC, electrochemistry; LC-MS/MS, liquid chromatography/tandem mass spectrometry; A, Adenosine; T, thrombin; LOD, limit of detection

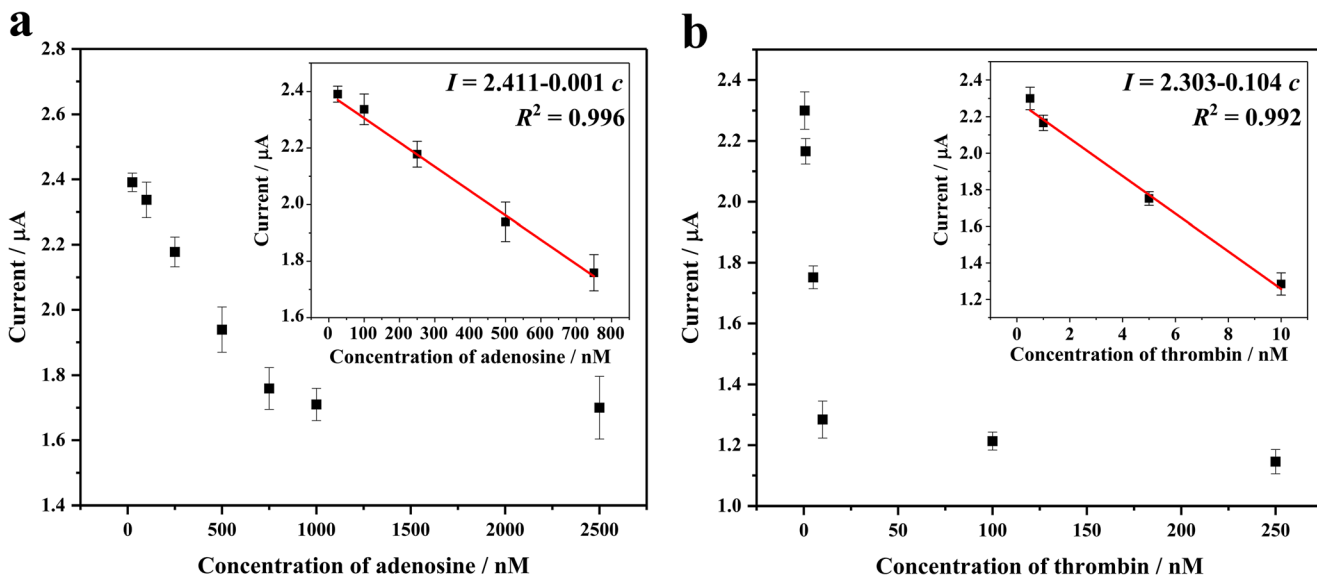


Fig. 6 Dependence of aptasensor response on **a** adenosine concentration (inset: calibration plot from 25 to 750 nM) and on **b** thrombin concentration (inset: calibration plot from 0.5 to 10 nM)

leads to larger surface area and fast electron transfer. However, the structure of ERGO will close-packed after excess deposition of ERGO nanosheets at GCE, resulting in reducing of effective surface area and blocking of electron movement [33, 34]. Additionally, loading amount of AuNPs on the surface of ERGO/GCE was determined by the electro-deposition time and also of great effect on performance of aptasensor. According to Fig. 5, the peak current starts to increase accompanied by extension of deposition time and reaches a maximum at 10 s, then decreases with further increment of deposition time. This phenomenon indicates that the film of AuNPs was too thin to be good for immobilization of aptamer when electrodeposition time was too short. On the contrary, excessive electrodeposition time might result in thick and tight film, thus decreasing the electron transfer. So, ERGO/GCE was prepared by CV with 10 cycles and electrodeposition time of AuNPs was 10 s.

Determination of adenosine and thrombin

This sensor was employed to determine adenosine and thrombin under optimal experimental conditions. Figure 6 displays the dependence of aptasensor response on the concentration of adenosine and thrombin. The peak current of MB decreased with increasing adenosine concentration and then hardly decreased when the concentration of adenosine increased to 2.5 μM (Fig. 6a), suggesting that the combination of aptamer and adenosine has achieved a balance at high concentration of adenosine and the amount of MB on aptamers remains unchanged. The inset illustrates that the calibration equation is $I (\mu A) = 2.411 - 0.001 c (nM)$ with a correlation coefficient R^2 of 0.996 for adenosine detection from 25 to 750 nM. The detection limit was 8.3 nM at a signal-to-noise ratio of 3. Similarly, according to Fig. 6b, a linear range from 0.5 to 10 nM is observed for thrombin detection with a detection limit

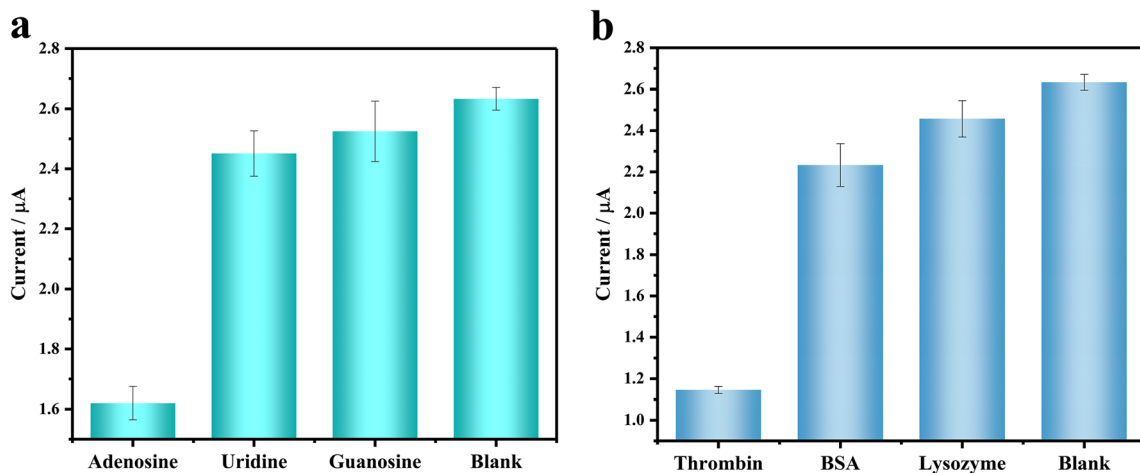


Fig. 7 Bar charts of DPV responses for **a** adenosine: adenosine, uridine, guanosine at 1 μM and **b** thrombin: thrombin, BSA, lysozyme at 300 nM

of 0.17 nM at a signal-to-noise ratio of 3 ($I = 2.303 - 0.104 c$, $R^2 = 0.992$). An analytical performance of our method is compared with previous works in Table 1, indicating success of our aptasensor.

Selectivity, reproducibility, and stability

Control experiments were carried out to study the specificity of this aptasensor. Uridine and guanosine belong to the nucleosides family and were used as reference substances to investigate their effects on the peak current of MB for determination of adenosine. The results are shown in Fig. 7a, the peak current of MB in the presence of 1 μ M uridine or guanosine exhibits a very small change compared with blank response. Meanwhile, BSA and lysozyme were used as interfering proteins to assess the specificity of sensor for thrombin detection. Figure 7b shows that there are no significant current response change when BSA or lysozyme is introduced. Thus, these results revealed the high selectivity of this aptasensor for adenosine and thrombin detection. The reproducibility of this sensor was examined by using five equally prepared electrodes. The relative standard deviations (RSD) were 2.6% for thrombin and 4.2% for adenosine, respectively. Moreover, the long-term storage stability of aptasensor was also tested. This aptasensor could retain over 90% of its initial current after a storage period of one week at 4 °C. These results showed that the aptasensor had good reproducibility and acceptable stability.

Conclusions

We have successfully proposed a simple and label-free electrochemical aptasensor for adenosine and thrombin detection using AuNPs-ERGO film modified GCE. The developed sensor is based on principle of switching structures of aptamers from DNA/DNA duplex to DNA/target complex using MB as an electrochemical indicator. During the concentration range of 25 nM to 750 nM for adenosine and 0.5 nM to 10 nM for thrombin, the peak currents show linear dependence with adenosine and thrombin concentration, and the limit of detection is respectively 8.3 nM and 0.17 nM. These experimental results indicate that the electrical conductivity of GO is significantly improved by electrochemical reduction. With the aid of AuNPs, electric characteristics and biocompatibility of sensing platform are further improved, which is beneficial to the performance of sensor. Moreover, the preparation method of AuNPs-ERGO film is very simple and economical. This aptasensor also exhibited a good selectivity for adenosine and thrombin due to the specific interactions between target and its aptamer. Finally, this method provides an option for dual-analyte detection of proteins and small molecules.

Funding This study is supported by the National Natural Science Foundation of China (21778041).

Declarations

Conflict of interest The authors declare that they have no conflict of interest.

References

- Zhang D, Ma JJ, Meng XW, Xu ZF, Zhang J, Fang YX, Guo Y (2019) Electrochemical aptamer-based microsensor for real-time monitoring of adenosine in vivo. *Anal Chim Acta* 1076:55–63
- Urbanová V, Jayaramulu K, Schneemann A, Kment Š, Fischer RA, Zbořil R (2018) Hierarchical porous fluorinated graphene oxide@metal-organic gel composite: label-free electrochemical aptasensor for selective detection of thrombin. *ACS Appl Mater Interfaces* 10(48):41089–41097
- Xu YY, Zhou WJ, Zhou M, Xiang Y, Yuan R, Chai YQ (2015) Toehold strand displacement-driven assembly of G-quadruplex DNA for enzyme-free and non-label sensitive fluorescent detection of thrombin. *Biosens Bioelectron* 64:306–310
- Chen ZB, Tan Y, Zhang CM, Yin L, Ma H, Ye NS, Qiang H, Lin YQ (2014) A colorimetric aptamer biosensor based on cationic polymer and gold nanoparticles for the ultrasensitive detection of thrombin. *Biosens Bioelectron* 56:46–50
- Man TT, Lai W, Xiao MS, Wang XW, Chandrasekaran AR, Pei H, Li L (2020) A versatile biomolecular detection platform based on photo-induced enhanced Raman spectroscopy. *Biosens Bioelectron* 147:111742
- Zhu Y, Hu XC, Shi S, Gao RR, Huang HL, Zhu YY, Lv XY, Yao TM (2016) Ultrasensitive and universal fluorescent aptasensor for the detection of biomolecules (ATP, adenosine and thrombin) based on DNA/Ag nanoclusters fluorescence light-up system. *Biosens Bioelectron* 79:205–212
- Zheng J, Li NX, Li CR, Wang XX, Liu YC, Mao GB, Ji XH, He ZK (2018) A nonenzymatic DNA nanomachine for biomolecular detection by target recycling of hairpin DNA cascade amplification. *Biosens Bioelectron* 107:40–46
- Zhang SS, Xia JP, Li XM (2008) Electrochemical biosensor for detection of adenosine based on structure-switching aptamer and amplification with reporter probe DNA modified Au nanoparticles. *Anal Chem* 80(22):8382–8388
- Jalil O, Pandey CM, Kumar D (2020) Electrochemical biosensor for the epithelial cancer biomarker EpCAM based on reduced graphene oxide modified with nanostructured titanium dioxide. *Microchim Acta* 187(5):275
- Zhou ZD, Gu CM, Chen C, Zhao PC, Xie YX, Fei JJ (2019) An ultrasensitive electrochemical sensor for quercetin based on 1-pyrenebutyrate functionalized reduced oxide graphene/mercapto- β -cyclodextrin/Au nanoparticles composite film. *Sensors Actuators B Chem* 288:88–95
- Hanko M, Švorc L, Planková A, Mikuš P (2019) Overview and recent advances in electrochemical sensing of glutathione—a review. *Anal Chim Acta* 1062:1–27
- Haque AMJ, Park H, Sung D, Jon S, Choi SY, Kim K (2012) An electrochemically reduced graphene oxide-based electrochemical immunosensing platform for ultrasensitive antigen detection. *Anal Chem* 84(4):1871–1878
- Shamsipur M, Farzin L, Tabrizi MA (2016) Ultrasensitive aptamer-based on-off assay for lysozyme using a glassy carbon electrode modified with gold nanoparticles and electrochemically reduced graphene oxide. *Microchim Acta* 183(10):2733–2743

14. Vinoth V, Wu JJ, Asiri AM, Anandan S (2017) Sonochemical synthesis of silver nanoparticles anchored reduced graphene oxide nanosheets for selective and sensitive detection of glutathione. *Ultrason Sonochem* 39:363–373
15. Fan LF, Zhang CY, Yan WJ, Guo YJ, Shuang SM, Dong C, Bi YP (2019) Design of a facile and label-free electrochemical aptasensor for detection of atrazine. *Talanta* 201:156–164
16. Ye YK, Yan WW, Liu YQ, He SD, Cao XD, Xu X, Zheng HS, Gunasekaran S (2019) Electrochemical detection of Salmonella using an invA genosensor on polypyrrole-reduced graphene oxide modified glassy carbon electrode and AuNPs-horseradish peroxidase-streptavidin as nanotag. *Anal Chim Acta* 1074:80–88
17. Yang SH, Zhang FF, Liang QL, Wang ZH (2018) A three-dimensional graphene-based ratiometric signal amplification aptasensor for MUC1 detection. *Biosens Bioelectron* 120:85–92
18. Yang JM, Li XL, Jiang BY, Yuan R, Xiang Y (2020) In situ-generated multivalent aptamer network for efficient capture and sensitive electrochemical detection of circulating tumor cells in whole blood. *Anal Chem* 92(11):7893–7899
19. Zhang LL, Zhang XY, Feng PJ, Han Q, Liu W, Lu Y, Song CX, Li FY (2020) Photodriven regeneration of G-Quadruplex aptasensor for sensitively detecting thrombin. *Anal Chem* 92(11):7419–7424
20. Qi LJ, Han X, Du Y (2020) Improved sensitivity for ratiometric fluorescence detection of ricin based on “kinetic competition” aptasensing strategy. *Sensors Actuators B Chem* 314:128073
21. Xiang WW, Lv QX, Shi HX, Xie B, Gao L (2020) Aptamer-based biosensor for detecting carcinoembryonic antigen. *Talanta* 214:120716
22. Tuerk C, Gold L (1990) Systematic evolution of ligands by exponential enrichment: RNA ligands to bacteriophage T4 DNA polymerase. *Science* 249(4968):505–510
23. Ellington AD, Szostak JW (1990) In vitro selection of RNA molecules that bind specific ligands. *Nature* 346(6287):818–822
24. So HM, Won K, Kim YH, Kim BK, Ryu BH, Na PS, Kim H, Lee JO (2005) Single-walled carbon nanotube biosensors using aptamers as molecular recognition elements. *J Am Chem Soc* 127(34):11906–11907
25. Liu JW, Lu Y (2006) Fast colorimetric sensing of adenosine and cocaine based on a general sensor design involving aptamers and nanoparticles. *Angew Chem Int Ed* 45(1):90–94
26. Centi S, Tombelli S, Minunni M, Mascini M (2007) Aptamer-based detection of plasma proteins by an electrochemical assay coupled to magnetic beads. *Anal Chem* 79(4):1466–1473
27. Zhu C, Li LS, Wang ZJ, Irfan M, Qu F (2020) Recent advances of aptasensors for exosomes detection. *Biosens Bioelectron* 160:112213
28. Ding LH, Wu YJ, Liu W, Liu L, Yu F, Yu SC, Tian YM, Feng JD, He LL (2019) Magnetic-assisted self-assembled aptamer/protein hybrid probes for efficient capture and rapid detection of cancer cells in whole blood. *Talanta* 205:120129
29. Xu YX, Bai H, Lu GW, Li C, Shi GQ (2008) Flexible graphene films via the filtration of water-soluble noncovalent functionalized graphene sheets. *J Am Chem Soc* 130(18):5856–5857
30. Shan CS, Yang HF, Song JF, Han DX, Ivaska A, Niu L (2009) Direct electrochemistry of glucose oxidase and biosensing for glucose based on graphene. *Anal Chem* 81(6):2378–2382
31. Zhu XH, Zeng LX, Xu MT, Liang Y, Nan JM (2012) A glassy carbon electrode modified with electrochemically reduced graphene for simultaneous determination of guanine and adenine. *Anal Methods* 4(9):2935–2939
32. Dong YP, Zhou Y, Wang J, Zhu JJ (2016) Electrogenated chemiluminescence resonance energy transfer between Ru(bpy)₃²⁺ electrogenerated chemiluminescence and gold nanoparticles/graphene oxide nanocomposites with graphene oxide as coreactant and its sensing application. *Anal Chem* 88(10):5469–5475
33. Edris NMMA, Abdullah J, Kamaruzaman S, Saiman MI, Sulaiman Y (2018) Electrochemical reduced graphene oxide-poly(eriochrome black T)/gold nanoparticles modified glassy carbon electrode for simultaneous determination of ascorbic acid, dopamine and uric acid. *Arab J Chem* 11(8):1301–1312
34. Yang SL, Lu ZZ, Luo SL, Liu CB, Tang YH (2013) Direct electrodeposition of a biocomposite consisting of reduced graphene oxide, chitosan and glucose oxidase on a glassy carbon electrode for direct sensing of glucose. *Microchim Acta* 180(1-2):127–135
35. Wang J, Li BZ, Lu QY, Li XY, Weng CY, Yan XQ, Hong JL, Zhou XM (2019) A versatile fluorometric aptasensing scheme based on the use of a hybrid material composed of polypyrrole nanoparticles and DNA-silver nanoclusters: application to the determination of adenosine, thrombin, or interferon-gamma. *Microchim Acta* 186(6):356
36. Feng CJ, Hou Z, Jiang W, Sang LH, Wang L (2016) Binding induced colocalization activated hybridization chain reaction on the surface of magnetic nanobead for sensitive detection of adenosine. *Biosens Bioelectron* 86:966–970
37. Sun JW, Jiang W, Zhu J, Li W, Wang L (2015) Label-free fluorescence dual-amplified detection of adenosine based on exonuclease III-assisted DNA cycling and hybridization chain reaction. *Biosens Bioelectron* 70:15–20
38. Xu SC, Man BY, Jiang SZ, Wang JH, Wei J, Xu SD, Liu HP, Gao SB, Liu HL, Li ZH, Li HS, Qiu HW (2015) Graphene/Cu nanoparticle hybrids fabricated by chemical vapor deposition as surface-enhanced Raman scattering substrate for label-free detection of adenosine. *ACS Appl Mater Interfaces* 7(20):10977–10987
39. Xu SC, Jiang SZ, Wang JH, Wei J, Yue WW, Ma Y (2016) Graphene isolated Au nanoparticle arrays with high reproducibility for high-performance surface-enhanced Raman scattering. *Sensors Actuators B Chem* 222:1175–1183
40. Sun QQ, Yan F, Su B (2018) Label-free electrochemical biosensors based on 3,3',5,5'-tetramethylbenzidine responsive isoporous silicamelle membrane. *Biosens Bioelectron* 105:129–136
41. Li F, Du ZF, Yang LM, Tang B (2013) Selective and sensitive turn-on detection of adenosine triphosphate and thrombin based on bifunctional fluorescent oligonucleotide probe. *Biosens Bioelectron* 41:907–910
42. Gao BB, Tang LTY, Zhang DG, Xie ZY, Su EB, Liu H, Gu ZZ (2017) Transpiration-inspired fabrication of opal capillary with multiple heterostructures for multiplex aptamer-based fluorescent assays. *ACS Appl Mater Interfaces* 9(38):32577–32582
43. Du F, Alam MN, Pawliszyn J (2014) Aptamer-functionalized solid phase microextraction-liquid chromatography/tandem mass spectrometry for selective enrichment and determination of thrombin. *Anal Chim Acta* 845:45–52

Publisher's note Springer Nature remains neutral with regard to jurisdictional claims in published maps and institutional affiliations.